Influence of mineral content and composition on graylevels in backscattered electron images of bone

John G. Skedros,[1] Roy D. Bloebaum,[1,*] Kent N. Bachus,[1] Todd M. Boyce,[1] and Brent Constantz[2]
[1]*Bone and Joint Research Laboratories (151F), VA Medical Center, 500 Foothill Blvd., Salt Lake City, UT 84148, and* [2]*Norian Corporation, 1025 Terra Bella Ave., Mountain View, CA 94043*

To determine the meaning of graylevels in backscattered electron (BSE) images of actual bone tissues, the influence of mineral content and mineral composition on BSE image graylevels was studied using chick bone tissue representing a broad age range. These tissues were analyzed for BSE image graylevels, Ca/P molar ratios, mineral composition, mineral content (v/v), ash fraction (w/w), and density (g/cm^3). Linear regression analyses showed that the weighted mean graylevels (WMGLs) in BSE images were positively correlated to ash fraction ($r^2 = 0.711$), mineral content ($r^2 = 0.720$), and density ($r^2 = 0.843$). Although the Ca/P ratio increased from 1.65 in embryos to 1.80 in 2-year olds, the compositional changes corresponding to this Ca/P molar ratio were estimated to produce a relatively minor (< 4.0%) change in BSE image graylevel. These results demonstrate that graylevels in BSE images of actual bone tissue can be attributed to mineral content and density, but only as a coincidence of their association with atomic number.

INTRODUCTION

Atomic-number-contrast backscattered electron (BSE) imaging is being developed into a useful tool in biomaterials interactions with bone and for determining and evaluating mineral content and density differences in bone tissue at the microscopic level.[1,2] The variations in the graylevels (shades of gray) in BSE images of bone tissue are considered to be directly related to variations in mineralization, and by implication, to variations in the mineral content and density (g/cm^3) of the imaged bone tissue.[1-3] However, it has been experimentally demonstrated that graylevels in BSE images of pure and composite materials are primarily dependent on atomic number.[1,2] Consequently, there is controversy surrounding interpretations that have assumed graylevels in BSE images of bone tissue to be directly related to variations in mineral content and/or density.[2] Using a simulated bone tissue model, a companion study has demonstrated that the graylevels in BSE images do indeed exhibit a strong positive correlation to average atomic number, as well as to mineral content and density.[2] If biomaterials investigators and basic bone researchers are to use BSE imaging technology for determining mineral content differences in bone tissue surrounding biomaterials at the microscopic level, further investigation is needed to verify that these fundamental relationships shown in simulated bone tissues are applicable to actual bone tissues. This verification is essential since it is not known whether graylevels in BSE images of bone tissue are influenced by maturation-related changes in the composition of the mineral component. These compositional changes can be the result of the incorporation or adsorption of various inorganic impurities in the mineral phase, the presence of various non-hydroxyapatite (HA) calcium-phosphate constituents, and/or with the crystallographic maturation or transformation of the predominant HA phase.[4-10]

A broad age range of chick tibial bone tissues, representing a broad range of mineralization, was selected for mineral composition, mineral content, and BSE image graylevel analysis. Chick tibial bone was selected for this study because age-related changes in composition of the organic matrix,[7] as well as those involving mineral content, composition, and crystallography have been well characterized.[5,8,11,12] Mineralization in the chick tibial diaphysis has been reported to occur before the 7th embryonic day and is

*To whom correspondence should be addressed.

Journal of Biomedical Materials Research, Vol. 27, 57–64 (1993)

CCC 0021-9304/93/010057-08

substantial by the 14th embryonic day.[11–13] Changes in the mineral content of this bone are known to occur at a rapid rate during the prehatching period[11,14]; during the prehatching period it has been estimated that bone mineral is remodeling so rapidly that the oldest age of the bone mineral is less than 48 h.[11] From the time of hatching (21st embryonic day) to about 10 weeks, continued mineralization results in increased average mineral content of lower limb bone tissue.[5] After 10 weeks, there is an attenuation in the rate of mineral accumulation and mineral content exhibits less than 5% increase from 10 weeks to 2 years.[5]

The objective of this study was to determine whether BSE image graylevels in actual bone tissues can be interpreted as a function of mineral content differences as previously demonstrated in simulated bone tissue.[2] It is hypothesized that mineral content differences will account for most (>90%) of the BSE image graylevel changes, and that associated changes in mineral composition will have a minimal to negligible role.

MATERIALS AND METHODS

White Leghorn 16–17 day embryonic, hatchling (1–2 day post-hatching), and 2-week-old chicks, and approximately 2-year-old female chickens were obtained from a local breeder. National Institutes of Health guidelines for the care and use of laboratory animals (NIH Publications #85–25 Rev. 1985) had been observed. Seven animals from each age group were sacrificed and their tibiae were immediately dissected free of periosteum and other soft tissues. One entire tibia from each of the embryos and hatchlings, the diaphysis of the 2-week-old chicks, and a 0.5-cm section from the middle third of the diaphysis from the 2-year-old chickens were embedded in polymethyl methacrylate (PMMA).[15] Contralateral tibial specimens were also obtained for tissue density, mineral content, and mineral composition analyses.

Embedded tibial specimens were fastened together with a cyanoacrylate glue to form one assembly of specimens. To maximize the bone surface area exposed to the electron beam, the specimens were arranged to expose longitudinal sections from the embryo, hatchling, and 2-week groups and mid-diaphyseal transverse sections of the 2-year-old tibiae. Pure magnesium and aluminum wires were inserted into holes that were drilled into the assembly. These metal standards were used for calibrating the scanning electron microscope (SEM).[16] The assembly was then ground, polished, gold-coated, and mounted for atomic-number-contrast BSE imaging according to methods described by Skedros et al.[2]

Image analysis

The image analysis system (Crystal, Link Analytical, Redwood City, CA), scanning electron microscope (JEOL JSM-T330A, JEOL USA, Inc., Peabody, MA), BSE detector (T300-BE152, JEOL Technics Ltd., Tokyo, Japan), and beam parameters used in this study have been described elsewhere.[2] Using ×200 magnification, three separate fields were indiscriminately selected along the diaphysis of each of the bones in each age group. The imaged bone tissues included periosteal and subperiosteal regions in all age groups. In the 2-year-olds, the imaged bone tissue was primarily compact bone. All images were obtained during one continuous imaging session using previously described image capture[2] and calibration methods.[16] Graylevel analyses of BSE images of the 2-week- and 2-year-old tibial bone tissues were systematically conducted using a grid system that was overlaid on the monitor of the image analysis system.[2] The grid system was not used for the BSE images of embryo and hatchling tibiae since they are highly porous and, consequently, a large portion of each image is occupied by regions consisting of marrow cavities filled with PMMA-infiltrated soft tissue. However, the analysis regions selected in these two age groups invariably sampled at least 70% of the bone tissue in each image.

The methods used to quantify BSE image graylevels have been described in detail by Bloebaum et al.[1] and Boyce et al.[16] The spectrum of graylevels in each analyzed region was graphically depicted as a graylevel histogram profile (GHP). For illustrative purposes, the individual GHPs, which represent individual analysis regions in images of each age group, were summed into one combined GHP.[2]

As described in a companion study,[2] all of the individual GHPs and the combined GHPs for each age group were assessed for their similarity in shape by visual inspection and by testing for skewness,[17] kurtosis,[17] and normality.[18] Visual inspection of all the GHPs demonstrated that they were continuous unimodal distributions that grossly resemble somewhat skewed Gaussian distributions. Weighted mean graylevels (WMGLs) were calculated from these GHPs using methods described in previous studies.[1,2,16]

Composition analysis

A 3- to 5-mm mid-diaphyseal section of bone tissue was obtained from each tibia contralateral to each of the embedded specimens. These sections were directly transferred to 70% ethanol, air dried for 5 min, and manually ground with an agate mortar and pestle. Approximately 10 mg of tissue was placed with 25 mg potassium bromide into the pestle and reground. These mixtures were pressed to a 12-mm

diameter by 2-mm-thick disk at 10,000 psi (68.95 MPa) and analyzed immediately on a Nicolett SDX Fourier transformed infrared (FTIR) spectrometer (Fremont, CA). This technique allows for the detection of various calcium phosphate crystal structures, and for compositional variations within each sample tested.[19]

Energy dispersive x-ray microanalysis was used to determine Ca/P molar ratios of the embedded bone tissues from each age group. These elements were selected because they have the greatest atomic number values of all the elements that are typically present in bone mineral. The analysis equipment included a Kevex x-ray detector (model 7000, Kevex Instruments, San Carlos, CA) interfaced to a JEOL JSM-35 scanning electron microscope (JEOL USA, Peabody, MA). Energy dispersive x-ray microanalysis was conducted on nine ×200 fields in each age group. The beam parameters consisted of 25 kV accelerating voltage, 90° incident angle, and 18° effective take-off angle.

Density and ash fraction

Tissue density was measured from bone samples adjacent to the sections obtained for the FTIR analyses. These samples were defatted under vacuum in a large volume of chloroform. After defatting the tissues, the chloroform was evaporated at 80°C and the tissues were placed in distilled water under vacuum (5 mm Hg) with constant stirring. Density was determined using described methods.[20,21] After the density measurements were obtained, the hydrated (postcentrifuged) bone was dried at 80°C for 4 days to achieve constant weight (< 1.0% change). The tissues were then allowed to cool for 6 h at room temperature in a desiccating chamber containing anhydrous $CaSO_4$ (Drierite, W.A. Hammond Drierite Co., Xenia, OH) and the weight of the dried bone was determined. The difference in weight between the dried bone and hydrated bone was taken to be the water content. The dried specimens were then placed into crucibles and were heated at 550°C for 24 h to remove organic constituents.[22] After heating, the ashed bone specimens were allowed to cool for 6 h at room temperature (20°C) in the desiccating chamber and were then removed from the crucibles and weighed to the nearest 0.00001 g on a analytical balance (Mettler H51, Mettler Instrument Corp., Hightstown, NJ). Ash fraction was calculated by dividing the weight of the ashed bone by the weight of the dried bone.

To compare the WMGL data to mineral content as defined in a companion study,[2] the averages of the measured weight fractions (w/w) of the mineral (ash), dry organic, and water components of each age group were converted to volume fractions (v/v) (Table I). The density used for these conversions was 3.18 g/cm^3 for the mineral (ash) component and 1.41 g/cm^3 for the dry organic component.[22] Using linear regression analyses, ash fraction, mineral content, and density data were compared to the WMGL data obtained for each age group.

Average atomic number of bone mineral and tissue

The average atomic number of the bone mineral component in each age group was calculated from mineral compositions that were obtained by using the following chemical formula, as described by Legros[10]: $Ca_{8.3}(PO_4)_{4.3}(CO_3)_x(HPO_4)_y(OH)_{0.3}$ where $(x + y)$ is constant and equal to 1.7. This stoichiometric relationship has been shown to approximate closely experimentally determined mineral compositions in rabbit, cat, rat, and human bone cortical bone tissue.[10] In each chick age group, the measured Ca/P molar ratios from the energy dispersive x-ray microanalysis study were used to establish the chemical formulas. Although these mineral compositions are different from stoichiometric HA, for our purposes they will be designated hereafter as HA. Using these HA mineral compositions, the average atomic numbers (Z) of the mineral components were determined using the

TABLE I
Measured Percentage of Ash, Weight Fractions, Calculated Volume Fractions, and Graylevel Data for the Tibial Bone Tissue in Each Age Group

Animal Age	% Ash (± SD)[a]	Weight Fractions [Volume Fraction][b] Mineral Fraction	Organic Fraction	Water Fraction	Density (± SD) (g/cm^3)	Average WMGL (± SD)
Embryo (n = 7)	56.6 (± 4.9)	0.47 [.26]	0.37 [.46]	0.16 [.28]	1.48 (± 0.09)	54.36 (± 6.25)
Hatched (n = 7)	57.9 (± 2.7)	0.50 [.31]	0.36 [.49]	0.14 [.20]	1.54 (± 0.33)	58.50 (± 8.69)
2 week (n = 7)	55.9 (± 3.7)	0.47 [.26]	0.37 [.46]	0.16 [.28]	1.61 (± 0.10)	65.94 (± 6.41)
2 year (n = 7)	72.5 (± 1.4)	0.65 [.42]	0.25 [.37]	0.10 [.21]	2.58 (± 0.33)	76.77 (± 15.34)

WMGL = weighted mean graylevel, SD = standard deviation.
[a]% Ash = ash weight/dry weight.
[b]Fraction by weight (w/w); volume fraction (v/v) calculated from the weight fractions. The volume fraction of the mineral component is considered to be mineral content.

weight fraction method described by Lloyd[23]:

$$\bar{Z} = \frac{\sum(NAZ)}{\sum(NA)} \quad (1)$$

where N is the number of atoms of each element with atomic weight A, atomic number Z, and $\sum(NA)$ is the molecular weight.

To assess the influence that the differences in mineral compositions might have on the atomic number of selected bone tissues, average atomic numbers were calculated for the bone tissue representing the embryo, hatchling, and 2-year-old groups. For the purposes of these calculations, bone tissue was considered to consist of three components: mineral, organic, and water. Since PMMA ($Z \approx 6.5$, $\rho = 1.8$ g/cm^3) is thought to replace much of the free water ($Z \approx 7$) during the vacuum-facilitated processing of bone tissue,[15] the free water fraction used in the calculations was considered to be entirely replaced with PMMA. The atomic number used for PMMA and the organic component was $Z = 6.5$, which was considered to be an appropriate estimate for the purpose of calculation, since both collagen and PMMA are primarily composed of carbon ($Z = 6$) with a considerable proportion of their atomic mass composed of oxygen ($Z = 8$). The average atomic number of the mineral, organic, and PMMA components were each multiplied by their respective weight fraction (Table I) and these values were summed to obtain an estimated average atomic number for the bone tissue in each of these three age groups.

RESULTS

The calibrated BSE images in Figure 1 illustrate the age- and mineral-content-related increases in graylevel brightness (Table I) in bone tissue from each of the four groups. Digital images similar to those shown in Figure 1 were obtained for use in the quantitative graylevel and Ca/P molar ratio analyses. The distributions of the combined GHPs of the four age groups (Fig. 2) demonstrate how the graylevel differences can be represented as unimodal distributions with their corresponding relative placements along the graylevel spectrum (abscissa). Analysis of variance (ANOVA) of the WMGLs (individual GHPs) (Table I) showed that they were significantly different ($P < .001$) in all possible pairings except for that between the embryo and hatchlings ($P = .11$). In contrast, the embryos, hatchlings, and 2-week-old group were not significantly different in terms of ash fraction ($P > .3$) or density ($P > .3$). This suggests that quantitative analysis of relative differences in BSE image graylevels could be a more sensitive technique for discerning relative mineral content differences in this animal model than are the conventional techniques used to measure ash fraction and density. Even though average densities of each group exhibited age-related increases, the average ash fraction of the 2-week-old chicks was lower than the average ash fractions of the embryo and hatchling groups (Table I). This apparent anomaly was thought to be attributable to the presence of marrow or other unrecognized volatile soft-tissue constituents that may have been retained during tissue processing.

Linear regression analyses showed that mineral content, defined in terms of volume percentages,[2] and ash fraction, defined in terms of weight percentages, were strongly correlated ($r^2 = 0.994$). Ash fraction also exhibited a positive correlation with density ($r^2 = 0.971$) which is the expected result based on previous studies.[14,24,25] Linear regression analysis showed that the averages of the WMGLs were positively correlated to ash fraction ($r^2 = 0.711$), mineral content ($r^2 = 0.720$), and density ($r^2 = 0.843$). Examination of the differences in WMGLs and densities between groups (Table I), suggests that density differences on the order of approximately 0.1 g/cm^3 may be discernible using these quantitative graylevel analysis and BSE imaging techniques.

The FTIR spectra obtained in the present study did not detect the presence of the low-atomic-number constituent, brushite (Table II), but did demonstrate the presence of very small amounts ($<< 1.0\%$) of a poorly crystalline HA-like phase in the embryonic tissues. This phase was similar to that which has previously been suggested to occur in these tissues.[12] FTIR spectra of the hatchling, 2-week-old, and 2-year-old groups revealed that the only detectable mineral phase present in their bone tissues was a highly crystalline HA. X-ray microanalysis showed that Ca/P molar ratio exhibited an increase from embryo to adult (Table II). Differences in the Ca/P molar ratios were not significant ($P > .05$) between the embryo and hatchling groups, but were significantly different for all other between-group comparisons ($P < .01$). Although the Ca/P molar ratio increased from hatchling (1.65) to 2-week-old (1.69) chicks, the calculated average atomic number remained almost constant (Table II). This demonstrates that increased Ca/P molar ratios do not invariably represent an increase in the atomic number of the mineral component. In the model studied, however, the increase in Ca/P molar ratio from embryo to hatchling was associated with an increase in average atomic number of the HA mineral component (Table II). However, the magnitude of the change in the Ca/P molar ratio did not parallel the increases demonstrated for average atomic number and WMGL between the bone tissue of the embryo and 2-year-old groups, where the 9.1% (1.65–1.80) increase in the Ca/P molar ratios corresponded to a 16.3% ($Z = 9.92$–11.54) increase in calculated average

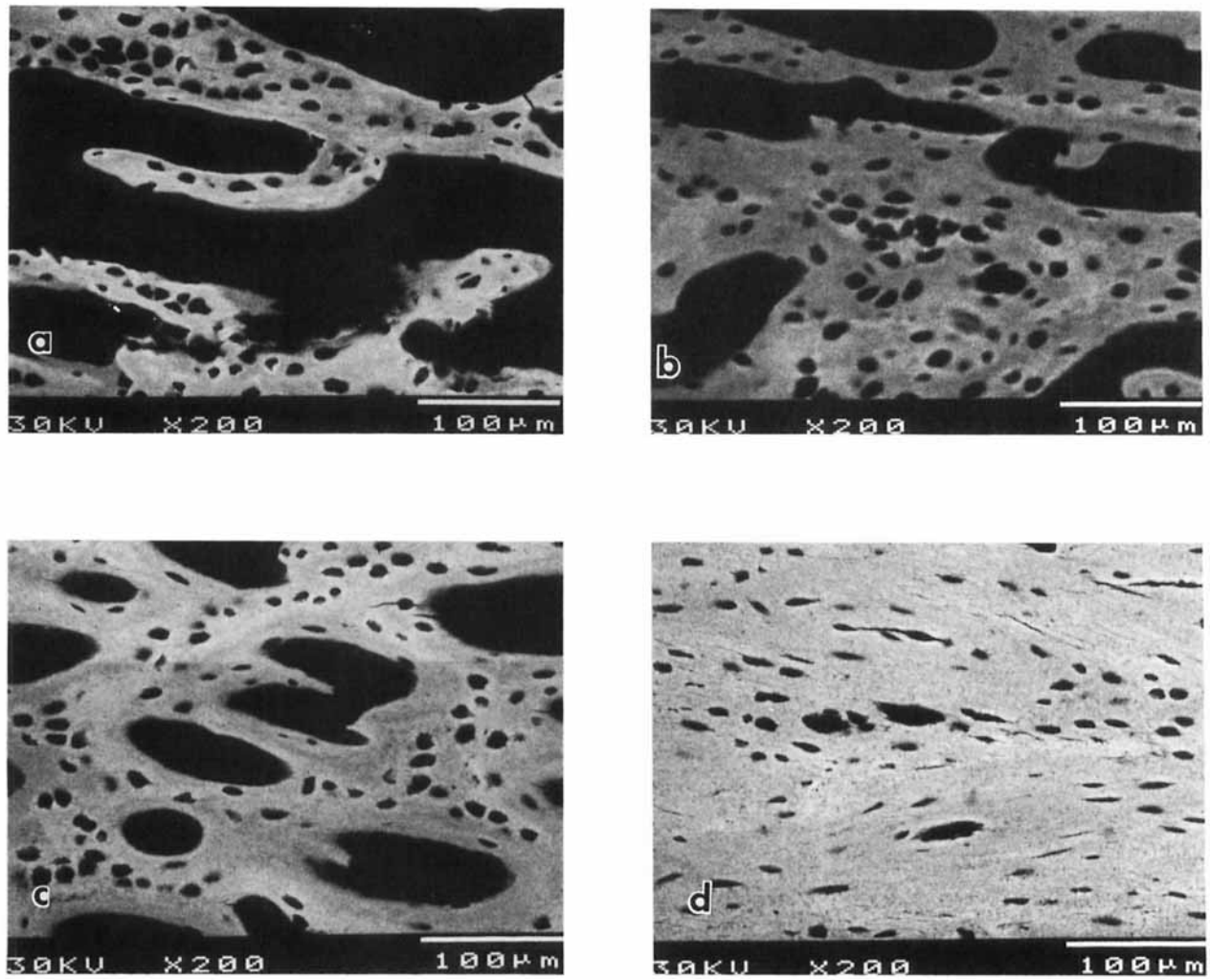

Figure 1. Backscattered electron images of representative fields of chick tibial bone tissue illustrating increasing graylevel brightness with increasing age (×200, 30 kV, 0° tilt): (a) embryo, (b) hatchling, (c) 2 week, and (d) 2 year. This increasing graylevel brightness was experimentally shown to be attributed to increasing mineral content, and is therefore indirectly related to increases in the density (g/cm^3) of the imaged bone tissue.

atomic number of the tissue and a 41.2% (54.36–76.77) increase in WMGL (Tables I and II).

DISCUSSION

The results of the present study demonstrate that WMGLs in BSE images of actual bone tissue exhibit strong positive correlations with mineral content and density. The proportional and fundamental relationship between WMGLs in BSE images to average atomic number of pure and composite materials has been established.[2,16] The positive correlations shown in this study between the BSE image graylevel differences of bone tissues and corresponding mineral content, ash fraction, and tissue density confirms the intimate relationship between these factors and their association with average atomic number.

The results of the x-ray compositional analysis are consistent with the findings of Pellegrino and Biltz,[25] who showed that maturation-related changes in the composition of the mineral component of chick diaphyseal bone tissue were manifested as increases in the Ca/P molar ratio. Since the atomic number of Ca ($Z = 20$) exceeds that of P ($Z = 15$), the progressive increase of the Ca/P molar ratio from embryo to 2-year-old might intuitively suggest a corresponding increase in the magnitude of the average atomic number. However, other elements may also be involved in bone mineral compositional changes that are associated with changes in the Ca/P ratio.[4] In addition, changes in the Ca/P molar ratio are not typically linked to increases in Ca ions per unit formula, but are attributed to decreases in orthophosphate ions (PO_4^{3-} and HPO_4^{2-}) resulting from substitutions or vacancies in the crystal lattice.[10] Consequently, changes in Ca/P molar ratios do not necessarily parallel the magnitude of the corresponding changes in the average atomic number of the mineral component. For example, if the bone tissues from the embryo and the 2-year-old

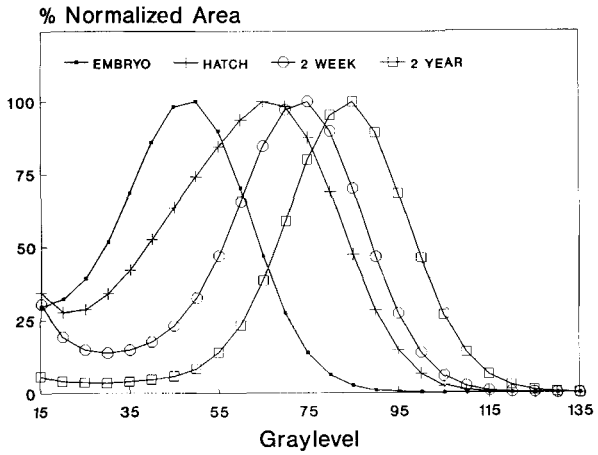

Figure 2. Combined graylevel histogram profiles representing all of the individual graylevel analyses conducted on the four age groups. The increase in graylevel intensity from embryo to 2-year-old bone tissue is seen as a shift in the relative position along the graylevel spectrum (abscissa).

age groups are considered to have equal mineral content, the 9.1% (1.65–1.80) increase in the Ca/P molar ratio between these two groups can be estimated to represent a rather small increase (< 3.0%) in average atomic number of the bone tissue. Based on the data in this study and on findings presented in a companion study,[2] it is suggested that this change in average atomic number would correspond to approximately a 4% increase in WMGL. This minor change in graylevel is near the threshold of what has been shown to be a detectable graylevel difference when using BSE image analysis techniques under SEM calibration conditions similar to those used in this study.[2] It can be concluded that the difference in the HA mineral composition between the embryo and 2-year-old may have contributed to the graylevel differences in the BSE images of these groups, but only to a minor degree.

Bone mineral composition data reviewed by LeGeros[4] further show that impurities typically occur in relatively small amounts. These results support the hypothesis that atomic number changes in bone tissue can be attributed primarily (> 90%) to increases in the mineral content, with maturation-related changes in mineral composition having a minimal (< 4.0%) to negligible (< 1.0%) role. These results are in agreement with the conclusions of a companion study in which it was suggested that graylevels in BSE images of actual bone tissue would primarily be a function of the relative degree of tissue mineralization.[2]

Results of the FTIR analysis showed that very small quantities of poorly crystalline HA are present only in embryonic bone tissue and that no other non-HA mineral phases or molecular impurities were detected in the tissue of the other age groups. These results further demonstrate that graylevels in BSE images of actual bone tissue are primarily dependent on variations in mineral content. Although changes in mineral composition that accompany bone tissue mineralization may only have a minor or negligible influence on atomic number contrast, it is possible that non-HA mineral phases or other variations in mineral composition may be present in pathologic and other types of mineralized tissues.[2,4] This possibility bespeaks the need to conduct correlated mineral compositional analysis whenever relative changes in BSE image graylevels might possibly be affected by differences in mineral composition.

Since bone tissue is essentially a composite of inorganic (mineral) and organic substances, the compositional changes of the organic matrix should also be considered in BSE image graylevel analysis. However, the carbonaceous composition of the organic matrix of bone tissue will most likely exhibit an average atomic number between $Z = 6$ and 7, and therefore would appear black with the SEM brightness, contrast, and spot size settings which are typically selected for BSE image graylevel analysis in bone tissue. Therefore, it is suggested that compositional changes associated with maturation and aging of the organic matrix probably, under most circumstances, have a negligible influence in altering graylevels in BSE images of bone tissue.

Examination of the density differences in Table I and the results of a companion study[2] suggest that quantitative analysis of graylevels in BSE images of bone tissue can be used to detect differences in mineral content which correspond to density differences on the order of approximately 0.1 g/cm^3. Because of the ability of these techniques to discern this relatively small mineral content change, BSE imaging technology should prove to be a useful tool for directly assessing temporal and spatial variations in the relative mineral content, and hence density, of bone tissue in discrete microscopic regions. In addition, because backscattered electrons sample between 1–5 μm of tissue depth in bone tissues,[26,27] BSE images can be used to conduct mineral content analyses on thick specimens of tissue with complex geometries, such as cancellous bone, which is not currently possible using other techniques.[28,29]

The biophysical basis for graylevel variations in BSE images of actual and simulated bone tissues, as clarified in this and in a companion study has been experimentally defined.[2] These studies will provide investigators with a conceptual foundation for future application of backscattered electron imaging techniques in determining relative differences in the bone mineral content at the interface with biomaterials at the microscopic level.

The authors acknowledge the support of the Department of Veterans Affairs Medical Center, Salt Lake City, UT, and the Whitaker Foundation. We thank Mark T. Nielsen for his

TABLE II
Molecular Formulas of the Hydroxyapatite-like Bone Mineral Compositions of the Four Age Groups Used in the Present Study, and of Pure Hydroxyapatite (HA) and Brushite

	Molecular Formulas	Average Z of Mineral	Ca/P Ratio (± SD)	Average Z of Tissue[a]
Age group				
Embryo	$Ca_{8.3}(PO_4)_{4.3}(CO_3)_{0.97}(HPO_4)_{0.73}(OH)_{0.3}$[b]	13.28	1.65 (0.04)	9.92
Hatchling	$Ca_{8.3}(PO_4)_{4.3}(CO_3)_{0.97}(HPO_4)_{0.73}(OH)_{0.3}$	13.78	1.65 (0.02)	10.14
2 week	$Ca_{8.3}(PO_4)_{4.3}(CO_3)_{1.09}(HPO_4)_{0.61}(OH)_{0.3}$	13.77	1.69 (0.07)	10.12
2 year	$Ca_{8.3}(PO_4)_{4.3}(CO_3)_{1.39}(HPO_4)_{0.31}(OH)_{0.3}$	14.26	1.80 (0.01)	11.54
Pure minerals				
HA	$Ca_{10}(PO_4)_6(OH)_2$	14.06	1.67	
Brushite	$CaHPO_4 \cdot 2H_2O$	11.85	1.0	

SD = standard deviation.

[a]The average atomic number of the bone tissue was estimated using the stoichiometric relationship described in the methods.

[b]HA mineral compositions were determined according to the methods of Legros et al. (ref. 10), as described in the text. HA compositions have the corresponding measured Ca/P molar ratios listed above.

Note. The embryo, hatchling, and 2-week chicks have nearly identical average atomic numbers and Ca/P molar ratios. The 2-year-old group shows compositional differences which would probably contribute to graylevel contrast observed in the BSE images. The far right column gives the calculated atomic numbers of bone tissue representing each age group.

helpful suggestions and Majna Plesko for her critical review. We also wish to acknowledge Gwenevere Shaw for her assistance in manuscript preparation and Cathy Sanderson for assistance with tissue processing.

References

1. R.D. Bloebaum, K.N. Bachus, and T.M. Boyce, "Backscattered electron imaging: The role in calcified tissue and implant analysis," *J. Biomater. Appl.*, **5**, 56–85 (1990).
2. J.G. Skedros, R.D. Bloebaum, K.N. Bachus, and T.M. Boyce, "The meaning of graylevels in backscattered electron images of bone," *J. Biomed. Mater. Res.*, **27**, 47–56 (1993).
3. S.A. Reid and A. Boyde, "Changes in the mineral density distribution in human bone with age: Image analysis using backscattered electrons in the SEM," *J. Bone Miner. Res.*, **2**, 13–22 (1987).
4. R.Z. LeGeros, "Apatites in biological systems," *Prog. Crystal Growth Charact.*, **4**, 1–45 (1981).
5. L.C. Bonar, A.H. Roufosse, W.K. Sabine, M.D. Grynpas, and M.J. Glimcher, "X-ray diffraction studies of the crystallinity of bone mineral in newly synthesized and density fractionated bone," *Calcif. Tiss. Int.*, **35**, 202–209 (1983).
6. J.M. Burnell, E.J. Teubner, and A.G. Miller, "Normal maturational changes in bone matrix, mineral, and crystal size in the rat," *Calcif. Tissue Int.*, **31**, 13–19 (1980).
7. J.B. Lian, A.H. Roufosse, B. Reit, and M.J. Glimcher, "Concentrations of osteocalcin and phosphoprotein as a function of mineral content and age in cortical bone," *Calcif. Tissue Int.*, **34**, S82–S87 (1982).
8. M. Grynpas and G. Hunter, "Bone mineral and glycosaminoglycans in newborn and mature rabbits," *J. Bone Miner. Res.*, **3**, 159–164 (1988).
9. F. Driessens and R. Verbeeck, "The dynamics of bone mineral in some vertebrates," *Z. Naturforsch.*, **41**, 468–471 (1986).
10. R. Legros, N. Balmain, and G. Bonel, "Age-related changes in mineral of rat and bovine cortical bone," *Calcif. Tissue Int.*, **41**, 137–144 (1987).
11. M.J. Glimcher, "The nature of the mineral component of bone and the mechanism of calcification," *Instr. Course Lect.*, **36**, 49–69 (1987).
12. D. Lee, W. Landis, and M. Glimcher, "The solid, calcium-phosphate mineral phases in embryonic chick bone characterized by high-voltage electron diffraction," *J. Bone Miner. Res.*, **1**, 425–432 (1986).
13. D.G. Pechak, M.J. Kujawa, and A.I. Caplan, "Morphology of bone development and bone remodeling in embryonic chick limbs," *Bone*, **7**, 459–472 (1986).
14. A. Roufosse, W. Landis, W. Sabine, and M. Glimcher, "Identification of brushite in newly deposited bone mineral from embryonic chicks," *J. Ultrastruc. Res.*, **68**, 235–255 (1979).
15. J. Emmanual, C. Hornbeck, and R.D. Bloebaum, "A polymethyl methacrylate method for large specimens of mineralized bone with implants," *Stain. Technol.*, **62**, 401–410 (1987).
16. T.M. Boyce, R.D. Bloebaum, K.N. Bachus, and J.G. Skedros, "Reproducible method for calibrating the backscattered electron signal for quantitative assessment of mineral content in bone," *Scan. Microsc.*, **4**, 591–603 (1990).
17. R.R. Sokal and F.J. Rohlf, *Biometry. The principles and practice of statistics in biological research*, W.H. Freeman & Co., New York, 1981.
18. J. Martinez and B. Iglewicz, "A test for departure from normality based on a biweight estimator of scale," *Biometrika*, **68**, 331–333 (1981).
19. C. Rey, J. Lian, M. Grynpas, F. Shapiro, L. Zylberberg, and M.J. Glimcher, "Non-apatitic environments in bone mineral: FT-IR detection, biological properties and changes in several disease states," *Connect. Tiss. Res.*, **21**, 267–273 (1989).
20. J.S. Arnold, "Quantitation of mineralization of bone as an organ and tissue in osteoporosis," *Clin. Orthop.*, **17**, 167–175 (1960).
21. D.B. Carter and W.D. Hayes, "The compressive behavior of bone as a two-phase porous structure," *J. Bone Jt. Surg.*, **59A**, 954–962 (1977).
22. J.K. Gong, J.S. Arnold, and S.H. Cohn, "The density of organic and volatile and non-volatile inor-

ganic components of bone," *Anat. Rec.*, **149,** 319–324 (1964).
23. G. E. Lloyd, "Atomic number and crystallographic contrast images with the SEM: a review of backscattered electron techniques," *Mineralog. Mag.*, **51,** 3–19 (1987).
24. R. M. Biltz and E. D. Pellegrino, "The chemical anatomy of bone," *J. Bone Jt. Surg.*, **51A,** 456–466 (1969).
25. E. Pellegrino and R. Biltz, "Mineralization in the chick embryo," *Calcif. Tissue Res.*, **10,** 128–135 (1972).
26. R. E. Holmes, H. K. Hagler, and C. A. Coletta, "Thick-section histometry of porous hydroxyapatite implants using backscattered electron imaging," *J. Biomed. Mater. Res.*, **21,** 731–739 (1987).
27. S. A. Reid, "A study of human skeletal maturation using the scanning electron microscope," Ph.D. Thesis, University College of London, 1986.
28. J. Jowsey, P. J. Kelly, B. L. Riggs, A. J. Bianco, D. A. Scholz, and J. Gershon-Cohen, "Quantitative microradiographic studies of normal and osteoporotic bone," *J. Bone Jt. Surg.*, **47A,** 785–806 (1965).
29. G. P. Vose, "Quantitative microradiography of osteoporotic compact bone," *Clin. Orthop.*, **24,** 206–212 (1962).

Received December 9, 1991
Accepted May 18, 1992